In vacuo photoemission study of atomically controlled $La_{1-x}Sr_xMnO_3$ thin films: Composition dependence of the electronic structure

K. Horiba,* A. Chikamatsu, H. Kumigashira,† and M. Oshima
Department of Applied Chemistry, The University of Tokyo, 7-3-1 Hongo, Bunkyo-ku, Tokyo 113-8656, Japan

N. Nakagawa and M. Lippmaa‡
Institute for Solid State Physics, The University of Tokyo, Kashiwa 277-8581, Japan

K. Ono
Institute of Materials Structure Science, High Energy Accelerator Research Organization (KEK), 1-1 Oho, Tsukuba 305-0801, Japan

M. Kawasaki‡
Institute for Materials Research, Tohoku University, Sendai 980-8577, Japan

H. Koinuma‡
Materials and Structures Laboratory, Tokyo Institute of Technology, Yokohama 226-8503, Japan
(Received 11 June 2004; revised manuscript received 8 November 2004; published 27 April 2005)

We have investigated change in the electronic structures of atomically controlled $La_{1-x}Sr_xMnO_3$ (LSMO) thin films as a function of hole-doping levels (x) in terms of *in vacuo* photoemission spectroscopy (PES) and x-ray absorption spectroscopy (XAS) measurements. The *in vacuo* PES measurements on a well-ordered surface of high-quality epitaxial LSMO thin films enable us to reveal their intrinsic electronic structures, especially the structure near the Fermi level (E_F). We found that overall the features of the valence band as well as the core levels monotonically shifted toward lower binding energy as x was increased, indicating the systematic chemical-potential shift of LSMO thin films with hole doping. The peak nearest to E_F due to the e_g orbital is also found to move toward E_F, while the peak intensity decreases with increasing x. The loss of spectral weight with x in the occupied density of states was compensated by the simultaneous increment of the shoulder structure in O 1s XAS spectra, suggesting the existence of a pseudogap, that is, a lowering in spectral weight at E_F, for all metallic compositions. These results indicate that the simple rigid-band model does not describe the electronic structure near E_F of LSMO, and that the spectral weight transfer from below to above E_F across the gap dominates the spectral changes with x in LSMO thin films.

DOI: 10.1103/PhysRevB.71.155420 PACS number(s): 79.60.−i, 71.30.+h

I. INTRODUCTION

Hole-doped manganese oxides with a perovskite structure of $Re_{1-x}Ae_xMnO_3$ (*Re* and *Ae* being trivalent rare earth and divalent alkaline earth elements, respectively) have attracted considerable attention, because they exhibit a rich phase diagram originating from the collective phenomena under the competition among different electronic phases due to the close interplay of spin, charge, orbital, and lattice degrees of freedom.[1,2] Among these manganites, $La_{1-x}Sr_xMnO_3$ (LSMO) thin films, which have been investigated here, is one of the most prototypical compounds. A parent compound $LaMnO_3$ is an antiferromagnetic insulator, while hole-doping induced by the substitution of Sr for La in the parent compound produces a ferromagnetic metallic phase[3] that shows colossal magnetoresistance (CMR). In addition to the CMR effect, the highest Curie temperature (T_C) of 360 K among manganites and its half metallic nature[4] make LSMO intriguingly attractive for potential applications to magnetoelectronic devices. Further hole-doping beyond the optimal doping level for ferromagnetic states ($x=0.4$) induces a transition from ferromagnetic metal to antiferromagnetic metal states for $x>0.5$.[5] In order to clarify the origin of these unusual physical properties, it is important to investigate how the electronic structures change as a function of hole-doping (Sr concentration x).

Photoemission spectroscopy (PES) has long played a central role in the measurement of the electronic structures of manganese oxides and their changes with carrier doping.[6–10] Nevertheless, recently questions arose as to reliability of PES spectra in addressing the bulk electronic structure of manganese oxides; the PES spectra of manganese oxides, especially the density of states (DOS) at the Fermi level (E_F), strongly depend on the surface preparation procedure as well as the experimental conditions. Since PES is quite a surface-sensitive technique, owing to short photoelectron mean-free paths, this may originate from different surface electronic structures induced by different surface preparations (scraping, fracturing, or sputtering and annealing) as well as different surface sensitivitities under different experimental conditions.[11] Although a large number of PES studies have been made on manganites, there is little agreement as to the hole-induced change in the electronic structure of LSMO. Furthermore, the metallic states of LSMO derived from the coherence of doped states may be deeply disturbed by the disorder induced by conventional surface preparations (for

example, in the scraped surface of polycrystalline samples).[12] Thus, in order to understand the bulk electronic structure, it is indispensable to perform the PES measurements on well-defined surfaces of manganese oxides.

In this paper, we report an *in vacuo* PES and x-ray absorption spectroscopic (XAS) study on the well-ordered surfaces of LSMO thin films grown by laser molecular beam epitaxy (laser MBE). The rapid progress in high-quality crystal growth techniques using laser MBE[13] has enabled us to grow LSMO thin films with atomically flat surfaces. We found that the valence-band spectra show significant difference between an atomically flat surface and a scraped one; in particular, the spectral weight of the Mn $3d$ e_g states closest to E_F is suppressed strongly in scraped surfaces. We also found that the spectra of ferromagnetic LSMO films ($x=0.4$) exhibit clear evidence for a Fermi cutoff, reflecting their metallic nature. This result clearly demonstrates the importance of an *in vacuo* PES study on a well-ordered surfaces of manganese oxides for revealing their intrinsic electronic structures. Combining the PES spectra and O $1s$ XAS spectra on the high-quality surface of LSMO thin films with various hole-doping levels, we have successfully obtained a picture of how the electronic structure evolves from an antiferromagnetic insulator to a ferromagnetic metal through the observation of the chemical-potential shift and spectral weight transfer near E_F.

II. EXPERIMENTAL SECTION

Our experiments were carried out using the high-resolution synchrotron radiation PES system combined with a laser MBE chamber,[14] which was installed at beamline BL-2C of the Photon Factory.[15] LSMO thin films were grown epitaxially on $SrTiO_3$ (STO) substrates by pulsed laser deposition. Sintered LSMO ($x=0$, 0.1, 0.2, 0.3, 0.4, and 0.55) pellets were used as ablation targets. A Nd: YAG laser was used for ablation in its frequency-tripled mode ($\lambda=355$ nm) at a repetition rate of 0.33 Hz. The wet-etched STO (001) substrates were annealed at 1050 °C at an oxygen pressure of 1×10^{-6} Torr before deposition in order to obtain an atomically flat TiO_2-terminated surface.[16] LSMO thin films with a thickness of about 400 Å were deposited on the TiO_2-terminated STO substrates at a substrate temperature of 950 °C and at an oxygen pressure of 1×10^{-4} Torr. The intensity of the specular spot in the reflection high-energy electron diffraction (RHEED) pattern was monitored during the deposition to determine the surface morphology and the film growth rate. The epitaxial growth of LSMO thin films on the STO substrate was confirmed by the observation of clear oscillations due to the layer-by-layer growth mode. The LSMO thin films were subsequently annealed at 400 °C for 30 min in the atmospheric pressure of oxygen to remove oxygen vacancies. After cooling to below 100 °C, the films were moved into the photoemission chamber under a vacuum of 10^{-10} Torr. The in-vacuum transfer was necessary to obtain the highest-quality surface as revealed by comparison with *ex situ* PES measurements.[14] The PES spectra were taken using the Gammadata Scienta SES-100 electron-energy analyzer. The measured spectra were momentum averaged because the analyzer acceptance angle is 15°, and it covers more than 1 Brillouin zone for a photoelectron with 600 eV kinetic energy. The total energy resolution at the photon energy of 600 eV was about 150 meV. The Fermi level of the samples was referred to that of a gold foil that was in electrical contact with the sample. The XAS spectra were obtained by measuring the sample drain current. The surface stoichiometry of the samples was carefully characterized by analyzing the relative intensity of relevant core levels, confirming that the composition of the samples was the same as that of the ceramic targets.[17] The surface morphology of the measured films was analyzed by *ex situ* atomic force microscopy (AFM) in air. The crystal structure was characterized by four-circle x-ray diffraction (4cXRD), confirming the epitaxial growth of the films on the substrates. The magnetization was measured by a superconducting quantum-interference device (SQUID) magnetometer with the magnetic field applied along the [100] axis parallel to the surface. The electorical resistivity was measured by the four-probe method.

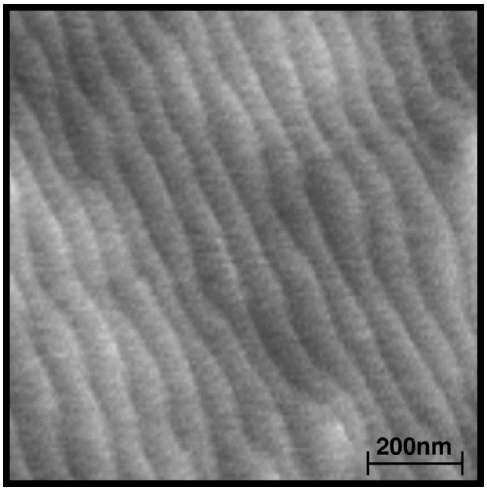

FIG. 1. A typical AFM image of a 400-Å-thick $La_{0.6}Sr_{0.4}MnO_3$ film grown on a $SrTiO_3$ (001) substrate.

III. RESULTS AND DISCUSSION

A. Physical properties of LSMO thin films

Figure 1 shows a typical AFM image of the fabricated LSMO, $x=0.4$ thin films. Atomically flat step-and-terrace structures which reflect the surface of STO substrates are clearly observed. The step height is measured to be about 0.4 nm, which is close to the c-axis constant of the LSMO films, indicating that film surfaces can be controlled on an atomic scale. Such atomically flat step-and-terrace structures are also observed in all the films reported here with different compositions, indicating the successful control of surface structure. Figure 2 shows the temperature dependence of electrical resistivity (ρ) for LSMO thin films with different compositions. The filled triangles indicate the T_C determined by magnetization measurement, which nearly agrees with those of the kink in the ρ-T curve. A significant change in ρ is observed at around T_C. Above $x=0.2$, metallic conduction

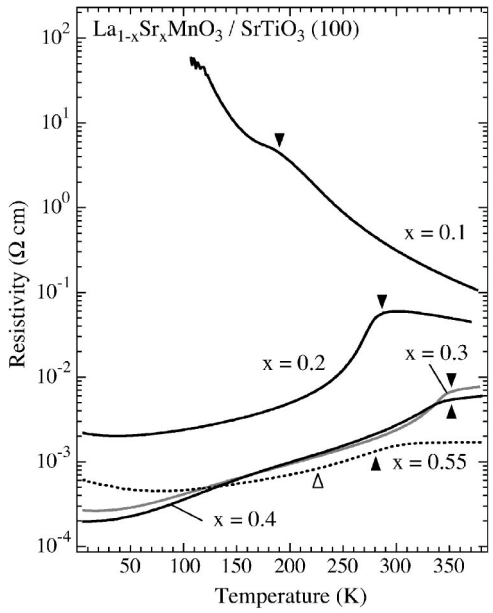

FIG. 2. Temperature dependence of resistivity for LSMO thin films. The filled triangles and an open triangle indicate the critical temperature for the ferromagnetic and antiferromagnetic phase transitions determined by the SQUID measurements, respectively.

is observed in the low-temperature ferromagnetic phase ($T < T_C$), whereas ρ at $x=0.1$ exhibits insulating behavior in all temperature ranges. Note that the ρ-T curve for $x=0$ films, as well as that for $x=0.1$ below 100 K, could not be measured, owing to the limitation of our ρ-T apparatus. In the high-temperature paramagnetic phase ($T > T_C$), the ρ-T curve is still characteristic of nonmetals (semiconductors), i.e., $d\rho/dT<0$, for $x=0.2$, the curve becomes metallic with further increasing $x>0.3$. The open triangles for $x=0.55$ indicate the critical temperature of the magnetic transitions from the ferromagnetic to the antiferromagnetic phase. We summarize in Table I the physical properties of the LSMO films. The obtained values are in good agreement with published data.[18–20]

B. Photoemission spectra on atomically-controlled LSMO films

Before proceeding to the compositional dependence of LSMO thin films, we first demonstrate the importance of

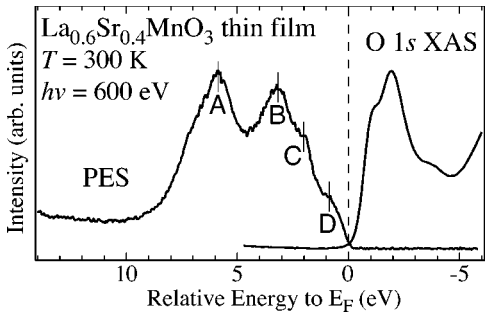

FIG. 3. PES and XAS spectra of $La_{0.6}Sr_{0.4}MnO_3$ thin films.

PES measurements on a well-ordered surface. Figure 3 shows an *in vacuo* photoemission spectrum combined with an O 1*s* XAS spectrum for the fabricated LSMO, $x=0.4$ thin film. The cleanliness of the surface required for PES measurements is confirmed by the absence of a hump structure around the binding energy of 8–10 eV. The hump structure is typically seen in the PES spectra on contaminated transition-metal-oxide surfaces.[7] The contamination-free surface is also confirmed by the fact that the "contamination" signal at the higher binding energy of the O 1*s* core level was negligibly weak, as shown in Fig. 6 later. In Fig. 3, the valence-band spectrum mainly consists of four structures, as labeled *A*, *B*, *C*, and *D*. In order to check the character of these features, we carried out Mn 2*p*-3*d* resonant PES (RPES) at various energies determined by the Mn 2*p* XAS profile, as shown in Fig. 4(a). Since the intensity of the structures *C* and *D* is resonantly enhanced at the photon energy around the Mn 2*p*-3*d* core threshold, as shown in Figs. 4(a) and 4(b), they originate from the Mn 3*d* states. In comparison with the cluster model calculation,[7] the *C* and *D* structures are assigned as the t_{2g} and e_g states, respectively. On the other hand, the two prominent structures (*A* and *B*) are the strongly mixed states of O 2*p* and Mn 3*d*.

The structure near E_F was not clearly observed in the previous PES studies on scraped surfaces of LSMO crystal[6,7] as well as those of other manganites,[21,22] where the spectral intensity near E_F is considerably suppressed. The strong enhancement of the near-E_F feature in the present study is not due to the difference in the photoionization cross section among the PES experiments, since the cross-section ratio between the Mn 3*d* and O 2*p* orbitals at the photon energy of

TABLE I. Physical properties of fabricated LSMO thin films. The T_C and the Néel temperature (T_N) are determined by the SQUID measurements. The out-of-plane (*c*-axis) and the in-plane (*a*-axis) lattice constants ($d_\perp$ and $d_\parallel$, respectively) are determined by the 4cXRD measurements.

x	T_C (K)	T_N (K)	$d_\perp$ (Å)	$d_\parallel$ (Å)	Ground state
0			3.949	3.892	
0.1	190	96	3.926	3.904	AFI
0.2	287		3.880	3.905	FM
0.3	352		3.855	3.905	FM
0.4	354		3.830	3.904	FM
0.55	281	226	3.803	3.889	AFM

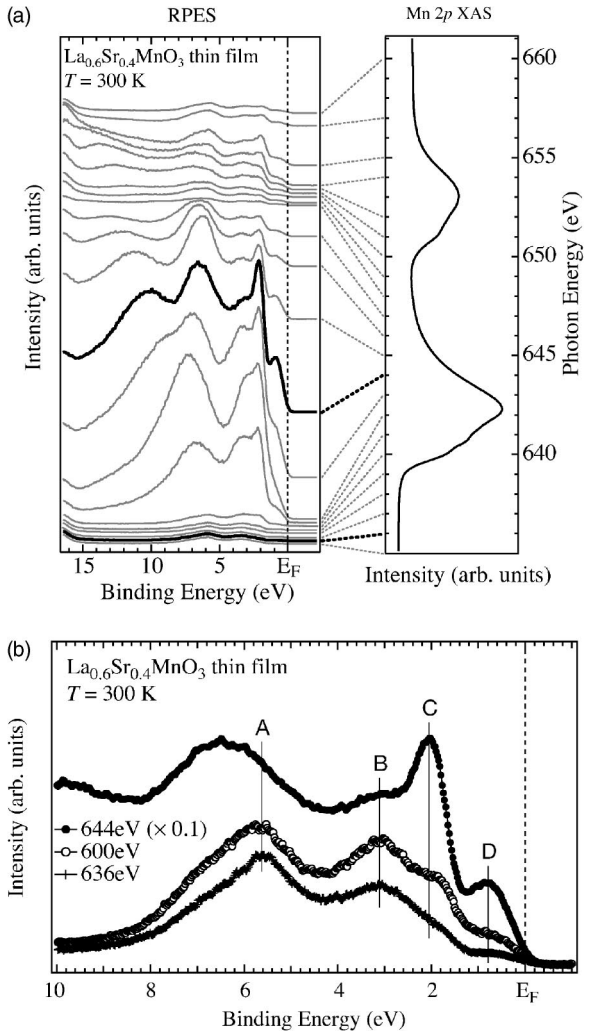

FIG. 4. (a) (Left) *In vacuo* Mn 2*p*-3*d* resonant PES spectra of $La_{0.6}Sr_{0.4}MnO_3$ thin films. The broken lines indicate the photon energy where the PES spectra were taken. The antiresonance (636 eV) and resonance (644 eV) spectra were shown with the black thick lines. (Right) The Mn 2*p* x-ray absorption spectrum of $La_{0.6}Sr_{0.4}MnO_3$ thin films. (b) A comparison between the antiresonance (crosses) and resonance (filled circles) PES spectra. The normal valence-band PES spectrum taken with a photon energy of 600 eV (open circles) is also shown.

600 eV is almost the same as that at the photon energy of 1253.6 eV (Mg Kα).[23] The influence of the energy resolution is also ruled out, since the previous PES results could not be reproduced by broadening our spectrum with a Gaussian function to simulate the difference in the energy resolution in each experiment. In contrast, the O 1*s* and Mn 2*p* XAS spectra, which have much deeper probing depths than those of PES measurements, are in good agreement with the scraped one.[24] Therefore, we conclude that the suppression of the spectral intensity near E_F may originate from the surface disorder induced by scraping or fracturing, indicating the importance of *in vacuo* PES measurements on well-ordered surfaces for revealing their intrinsic electronic structures.

The next crucial issue is whether the Fermi edge is clearly observed or not. In order to investigate the electronic

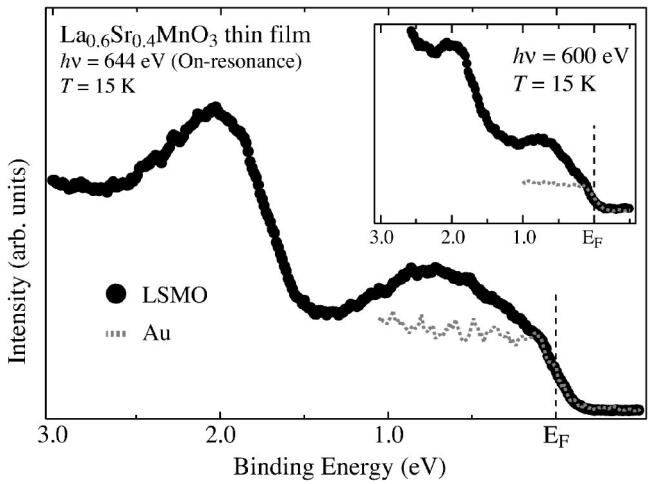

FIG. 5. High-resolution resonant PES spectrum of $La_{0.6}Sr_{0.4}MnO_3$ thin films (filled circles) and photoemission spectrum of gold (broken line) near E_F at 15 K. The inset shows the nonresonant PES spectrum measured with $h\nu$=600 eV at 15 K.

structure near E_F in more detail, we have measured the Mn 2*p*-3*d* resonant PES spectra near E_F with higher energy resolution at low temperature. Figure 5 shows the high-resolution Mn 2*p*-3*d* RPES (HRRPES) spectrum of the LSMO, x=0.4 thin films. We find that the HRRPES spectrum exhibit a sharp increase of intensity at E_F with decreasing temperature and a clear Fermi-edge profile at low temperature, reflecting the metallic ground states of LSMO, x=0.4 thin films. The existence of a Fermi edge is more clearly seen by comparison with the spectrum of gold. The clear Fermi edge is also observed in the nonresonant spectra at 15 K, as shown in the inset of Fig. 5. This result is a sharp contrast to the previous PES results, where the spectral weight near E_F is considerably suppressed and, consequently, the Fermi edge is hardly seen,[6,7] even at low temperature.[8,9] The suppression may originate from the surface disorder induced by conventional surface-preparation procedures (scraping or fracturing) in the conventional PES measurements, since the metallic state of LSMO results from the coherence of doped states, which may be deeply disturbed by the disorder. In fact, the physical properties of manganites are considerably sensitive to the structural disorder.[2] These results strongly suggest the importance of *in vacuo* PES measurements on a well-ordered surface of transition metal oxides for revealing their intrinsic electronic structures.

C. Compositional dependence of core-level PES spectra

Next, we discuss how the electronic structure changes as a function of hole doping. Figure 6 shows the Sr-concentration dependence of the core-level PES spectra obtained from well-ordered surfaces of LSMO thin films. The peak positions of La 4*d*, Sr 3*d*, and O 1*s* core levels were determined by a curve fitting as indicated by vertical lines in Figs. 6(a), 6(b), and 6(c), respectively. These core levels monotonically shift toward lower binding energies with increasing x. The monotonic peak shift may reflect the chemical-potential shift of LSMO with hole doping. For the Mn 2*p* core levels, we

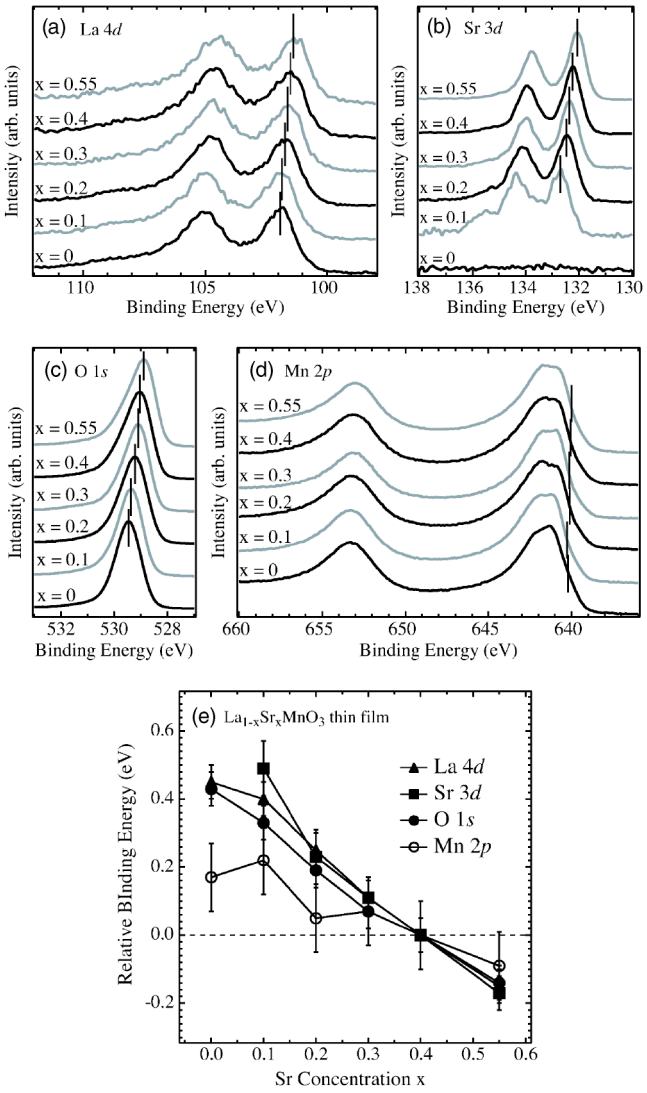

FIG. 6. Composition dependence of the (a) La 4*d*, (b) Sr 3*d*, (c) O 1*s*, and (d) Mn 2*p* core-level PES spectra of LSMO thin films measured with $h\nu$=800 eV at 300 K. (e) The composition dependence of the peak positions of the core-level PES spectra. We estimate the peak positions of the La 4*d*, Sr 3*d*, and O 1*s* core levels by fitting them with a Gaussian function, and the peak positions of the Mn 2*p* core levels from the midpoint of the lower binding-energy slope, as indicated by vertical lines in Figs. 6(a), 6(b), 6(c), and 6(d), respectively.

estimated the peak positions from the midpoint of a leading edge, as indicated by the vertical lines in Fig. 6(d), since it is difficult to determine the peak positions of the Mn $2p_{3/2}$ core levels, owing to the existence of Mn^{3+} and Mn^{4+} multiplets. The estimation of the energy shift from Mn $2p_{1/2}$ peaks gave nearly the same results. The deviation of the peak shift for Mn 2*p* core levels with respect to other core levels may be attributed to the increase in the Mn valence from Mn^{3+} to Mn^{4+} with hole doping, i.e., to the so-called chemical shift. All core levels were found to shift by the same amount toward lower binding energies with increasing Sr concentration, reflecting a monotonic chemical-potential shift with Sr concentration, as summarized in Fig. 6(e). The monotonic core-level shift with hole doping seems to be a common

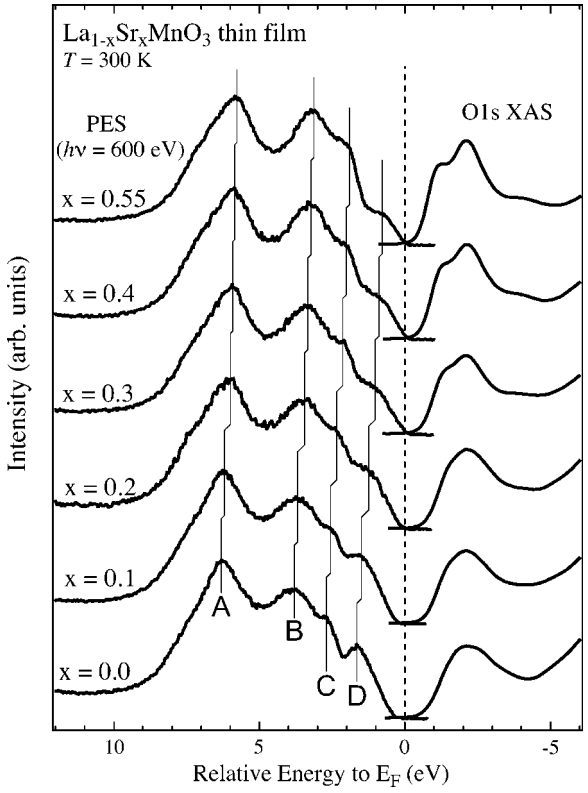

FIG. 7. Composition dependence of the valence-band PES ($h\nu$ =600 eV) and O 1*s* XAS spectra of LSMO thin films. The peak positions indicated with vertical lines are determined by the fitting of each spectrum with Gaussian components. The energies of the XAS spectra were referenced to the optical gap of $LaMnO_3$ reported by Arima *et al.*[27] and the *x*-dependent shift of the O 1*s* core-level peak in our PES measurements.

phenomenon in hole-doped manganite oxides.[10,21] The linear dependence on chemical-potential shift as a function of *x* is in contrast with the results on $La_{2-x}Sr_xCuO_4$ (LSCO) (Ref. 25) and $La_{1-x}Sr_xFeO_3$ (LSFO),[26] where the significant suppression of the chemical-potential shift has been observed in the underdoped region of LSCO and in the charge-ordered phase of LSFO, respectively. These phenomena have been attributed to the formation of charge stripe for LSCO and the charge disproportion for LSFO, which are kinds of "microscopic phase separations." Since the electronic phase separation results in the pinning of the chemical potential, the monotonic chemical-potential shift of LSMO suggests the absence of phase separation on a microscopic scale.[10]

D. Compositional dependence of valence-band PES spectra

Figure 7 shows the Sr-concentration dependence of the combined valence-band PES spectra and O 1*s* XAS spectra. Here, O 1*s* XAS spectra for $LaMnO_3$ have been aligned so that the gap magnitude agrees with that obtained from the optical measurements, 1.1 eV,[27] since the E_F position for O 1*s* XAS cannot be determined unambiguously from the O 1*s* core-level PES and XAS data, because of the unknown effect of the core-hole potential.[7] The Fermi levels of the XAS spectra for other compositions were determined by combin-

ing the Fermi-level position in the $LaMnO_3$ spectrum with the x-dependent shift of the O 1s core-level peak, for the sake of convenience. In the valence-band PES spectra for all compositions, we immediately notice that the features closest to E_F are clearly observed in contrast to the previous PES results. Especially for $LaMnO_3$, the e_g-derived structure closest to E_F is remarkably enhanced in comparison with the previous PES results.[6,7,21] The presence of such an e_g-derived feature in the valence-band spectra of $LaMnO_3$ is predicted by the recent band-structure calculation considering the photoemission-final-state effect correctly.[28] The overall features of the present PES spectrum of $LaMnO_3$ show good agreement with this calculation. In addition, we find that there is hardly any intensity in PES spectrum of $LaMnO_3$ at E_F, which is consistent with the insulating ground state of $LaMnO_3$. The absence of spectral weight within the band gap of $LaMnO_3$ suggests that the influence of excess oxygen in $LaMnO_3$ is negligible.

With hole doping by substitution of Sr for La in LSMO, systematic changes in the electronic structures were observed. It was found that all structures of the valence-band PES spectra monotonically shift toward lower binding energies with increasing Sr concentration, which is the same for the core-level spectra. On the other hand, the peak intensity of the feature D systematically decreases with increases in the Sr concentration x, while the intensity of the other features at higher binding energies seems to be preserved. Compensating for the loss of spectral weight, a shoulder structure near E_F in the O 1s XAS spectra simultaneously increases, suggesting the spectral weight transfer across a gap or pseudogap[29] at E_F.

Figure 7 shows that features A, B, and C shift in energy position, but do not change significantly in intensity, while the e_g state (feature D) shows a systematic change in intensity and peak position. In order to investigate the change in the e_g state as a function of the hole-doping level in more detail, we extract the e_g states by subtracting the contribution from the other states which are simulated by a linear combination of Gaussian functions and an integral background. The results are shown in Fig. 8(a). It is clearly observed that the peak shift and the reduction of spectral weight occur in the e_g states at the same time. Assuming that the hole was doped into the e_g states mainly, the spectral weight should be proportional to the filling of the e_g states $(1-x)$. In Fig. 8(b), we plot the relative spectral weight of the e_g states as a function of hole concentraton, confirming a linear relation between the spectral weight and the filling of the e_g states.

The energy shifts in the valence-band features are summarized in Fig. 8(c), together with the average of the peak shifts in the La 4d, Sr 3d, and O 1s core levels. As expected, these energy shifts are almost the same as each other, indicating the systematic chemical-potential shift of LSMO thin films with hole doping. The observed monotonic shift of the energy position of the e_g states is different from that in the previous PES studies on LSMO polycrystalline samples, where the energy shift of the e_g states got pinned in the metallic region of LSMO,[7] although a monotonic chemical-potential shift for core levels was observed.[10,21] The discrepancy in energy shifts among experiments may stem from the difficulty in determining the energy position accurately in the conventional PES measurements due to the considerable suppression of spectral weight for the e_g states. Again, the reasonable spectral behavior with doping demonstrates that the high-quality spectra showing the intrinsic spectral features in LSMO are successfully obtained from the present PES studies on well-ordered surfaces.

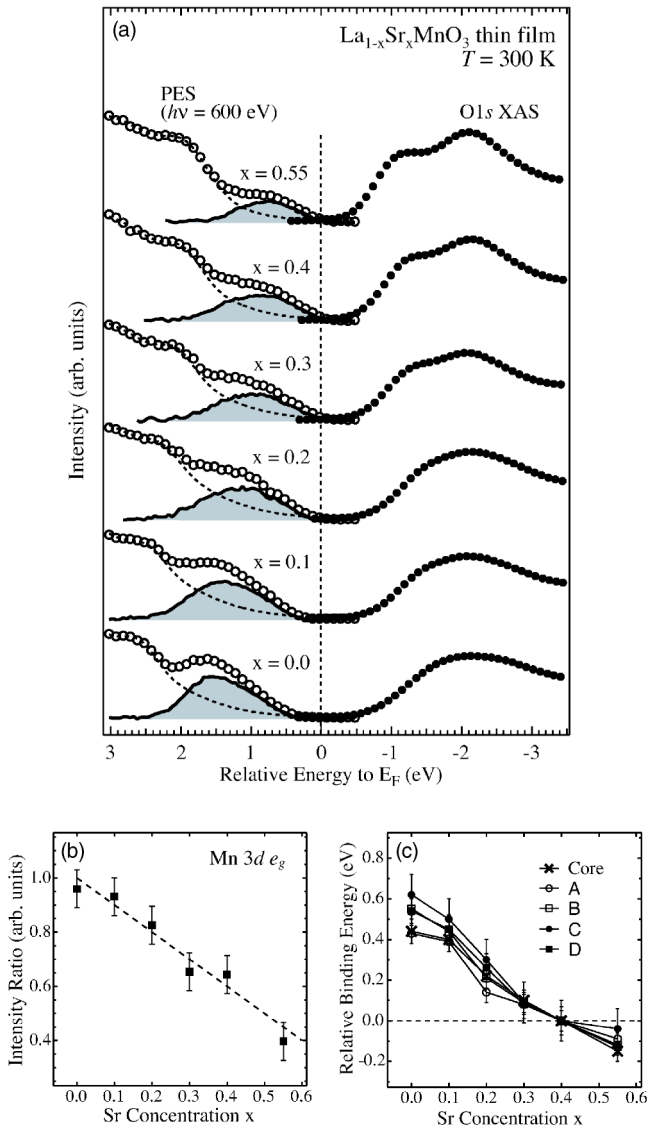

FIG. 8. (a) The expansion graph of the valence-band PES spectra (open circles) and XAS spectra (filled circles) near E_F, and the extracted e_g states (solid lines) obtained by subtracting the contribution from the other states (dotted lines) from the valence-band PES spectra. For details, see the text. (b) The peak area of the extracted e_g states plotted as a functions of Sr concentration x. A broken line shows the hole concentrations of these compounds. (c) The composition dependence of the peak positions of the valence-band PES spectra as well as the core levels.

Finally, we discuss the redistribution of spectral weight near E_F. In the rigid-band picture, it is expected that the peak intensity itself does not change unless the peak top crosses E_F. However, the peak intensity of the e_g states decreases linearly with hole doping, as shown in Fig. 8(a), together with the simultaneous increase in intensity for shoulder

structures near the leading edge of O 1*s* XAS spectra. These results indicate that the "nonrigid-bandlike" behavior occurs at the near-E_F region, where a gap or pseudogap is opened at E_F and, consequently, the spectral weight is redistributed between the occupied states and unoccupied states with hole-doping.[25] The systematic spectral-weight transfer across E_F is clearly seen in the combined PES and XAS spectra. This nonrigid-band behavior near E_F is apparently in conflict with the monotonic chemical-potential shift. We therefore conclude that the effect of hole-doping on the electronic structure of LSMO can be described in the systematic chemical-potential shift in terms of the energy positions of core-level and valence states, whereas the e_g states also show nonrigid-bandlike behavior in terms of the spectral weight transfer from below to above E_F across the gap or pseudogap at E_F.

IV. CONCLUSION

We have performed *in vacuo* synchrotron-radiation photoemission measurements on the well-ordered surfaces of LSMO thin films to investigate change in the electronic structures of LSMO thin films as a function of the hole concentration x. The PES spectra for the laser-MBE-grown samples clearly show that the intensity of the e_g states closest to E_F is significantly enhanced for well-ordered surfaces grown by laser MBE. Furthermore, the high-resolution Mn $2p-3d$ resonant PES spectra for metallic LSMO, $x=0.4$ thin films exhibit the clear evidence of a Fermi cutoff, which is not clearly observed in the previous PES measurements. These results clearly indicate the importance of an *in vacuo* PES study on a well-ordered surface of transition metal oxides. Combining the PES spectra and the O 1*s* XAS spectra on the well-ordered surfaces of LSMO thin films, we successfully obtained a picture of how the electronic structures evolve as functions of hole concentration x. We found that the overall features of the valence-band as well as the core levels monotonically shifted toward lower binding energies as x was increased, indicating the systematic chemical-potential shift of LSMO thin films with hole doping. In the PES spectra near E_F, the e_g-derived structure becomes weaker and moves toward E_F as x is increased. The linear relation between the spectral weight and the filling for the e_g states reveals that the holes are doped into the e_g states. The pseudogap, which is a depression in spectral weight at E_F, exists for all metallic compositions. These results indicate that the simple rigid-band model does not describe the electronic structure of LSMO and the spectral weight transfer occurs across E_F in a nonrigid-bandlike manner.

ACKNOWLEDGMENTS

We thank Professor A. Fujimori and Dr. A. Chainani for helpful discussions. This work has been done under Project No. 02S2-002 at the Institute of Material Structure Science at KEK.

*Present address: RIKEN/SPring-8, 1-1-1 Kouto, Mikazuki-cho, Sayo-gun, Hyogo 679-5148, Japan.

†Author to whom correspondence should be addressed. Electronic address: kumigashira@sr.t.u-tokyo.ac.jp

‡Also at Combinatorial Materials Exploration and Technology (COMET), Tsukuba 305-0044, Japan.

[1] M. Imada, A. Fujimori, and Y. Tokura, Rev. Mod. Phys. **70**, 1039 (1998).

[2] *Colossal Magnetoresistive Oxides*, edited by Y. Tokura, Advances in Condensed Matter Science, Vol. 2 (Gordon and Breach, Amsterdam, 2000).

[3] A. Urushibara, Y. Moritomo, T. Arima, A. Asamitsu, G. Kido, and Y. Tokura, Phys. Rev. B **51**, 14 103 (1995).

[4] J.-H. Park, E. Vescovo, H. J. Kim, C. Kwon, R. Ramesh, and T. Venkatesan, Nature (London) **392**, 794 (1998).

[5] H. Fujishiro, M. Ikebe, and Y. Konno, J. Phys. Soc. Jpn. **67**, 1799 (1998).

[6] A. Chainani, M. Mathew, and D. D. Sarma, Phys. Rev. B **47**, 15 397 (1993).

[7] T. Saitoh, A. E. Bocquet, T. Mizokawa, H. Namatame, A. Fujimori, M. Abbate, Y. Takeda, and M. Takano, Phys. Rev. B **51**, 13 942 (1995).

[8] D. D. Sarma, N. Shanthi, S. R. Krishnakumar, T. Saitoh, T. Mizokawa, A. Sekiyama, K. Kobayashi, A. Fujimori, E. Weschke, R. Meier, G. Kaindl, Y. Takeda, and M. Takano, Phys. Rev. B **53**, 6873 (1996).

[9] T. Saitoh, A. Sekiyama, K. Kobayashi, T. Mizokawa, A. Fujimori, D. D. Sarma, Y. Takeda, and M. Takano, Phys. Rev. B **56**, 8836 (1997).

[10] J. Matsuno, A. Fujimori, Y. Takeda, and M. Takano, Europhys. Lett. **59**, 252 (2002).

[11] A. Sekiyama, T. Iwasaki, K. Matsuda, Y. Saitoh, Y. Onuki, and S. Suga, Nature (London) **403**, 396 (2000).

[12] K. Breuer, S. Messerli, D. Purdie, M. Garnier, M. Hengsberger, Y. Baer, and M. Mihalik, Phys. Rev. B **56**, R7061 (1997).

[13] H. Koinuma, N. Kanda, J. Nishino, A. Ohtomo, H. Kubota, M. Kawasaki, and M. Yoshimoto, Appl. Surf. Sci. **109/110**, 514 (1997).

[14] K. Horiba, H. Ohguchi, H. Kumigashira, M. Oshima, K. Ono, N. Nakagawa, M. Lippmaa, M. Kawasaki, and H. Koinuma, Rev. Sci. Instrum. **74**, 3406 (2003).

[15] M. Watanabe, A. Toyoshima, Y. Azuma, T. Hayaishi, Y. Yan, and A. Yagishita, Proc. SPIE **3150**, 58 (1997).

[16] M. Kawasaki, K. Takahashi, T. Maeda, R. Tsuchiya, M. Shinohara, T. Yonezawa, O. Ishihara, M. Yoshimoto, and H. Koinuma, Science **266**, 1540 (1994).

[17] H. Kumigashira, K. Horiba, H. Ohguchi, K. Ono, M. Oshima, N. Nakagawa, M. Lippmaa, M. Kawasaki, and H. Koinuma, Appl. Phys. Lett. **82**, 3430 (2003).

[18] M. Izumi, Y. Konishi, T. Nishihara, S. Hayashi, M. Shinohara, M. Kawasaki, and Y. Tokura, Appl. Phys. Lett. **73**, 2497 (1998).

[19] M. Izumi, T. Manako, Y. Konishi, M. Kawasaki, and Y. Tokura, Phys. Rev. B **61**, 12 187 (2000).

[20] T. Fukumura, M. Ohtani, M. Kawasaki, Y. Okimoto, Y. Tokura,

and H. Koinuma, Appl. Phys. Lett. **77**, 3426 (2000).
[21] J.-H. Park, C. T. Chen, S.-W. Cheong, W. Bao, G. Meigs, V. Chakarian, and Y. U. Idzerda, Phys. Rev. Lett. **76**, 4215 (1996).
[22] A. Sekiyama, S. Suga, M. Fujikawa, S. Imada, T. Iwasaki, K. Matsuda, T. Matsushita, K. V. Kaznacheyev, A. Fujimori, H. Kuwahara, and Y. Tokura, Phys. Rev. B **59**, 15 528 (1999).
[23] J. J. Yeh and I. Lindau, At. Data Nucl. Data Tables **32**, 1 (1985).
[24] M. Abbate, F. M. F. de Groot, J. C. Fuggle, A. Fujimori, O. Strebel, F. Lopez, M. Domke, G. Kaindl, G. A. Sawatzky, M. Takano, Y. Takeda, H. Eisaki, and S. Uchida, Phys. Rev. B **46**, 4511 (1992).
[25] A. Fujimori, A. Ino, J. Matsuno, T. Yoshida, K. Tanaka, and T. Mizokawa, J. Electron Spectrosc. Relat. Phenom. **124**, 127 (2002).
[26] H. Wadati, D. Kobayashi, H. Kumigashira, K. Okazaki, T. Mizokawa, A. Fujimori, K. Horiba, M. Oshima, N. Hamada, M. Lippmaa, M. Kawasaki, and H. Koinuma, Phys. Rev. B **71**, 035108 (2005).
[27] T. Arima, Y. Tokura, and J. B. Torrance, Phys. Rev. B **48**, 17 006 (1993).
[28] P. Ravindran, A. Kjekshus, H. Fjellvåg, A. Delin, and O. Eriksson, Phys. Rev. B **65**, 064445 (2002).
[29] The "pseudogap" corresponds to the ferromagnetic metallic phase which exhibits suppressed intensity at or near E_F at 300 K, but the data in Fig. 5 show a clear Fermi edge at low temperature.